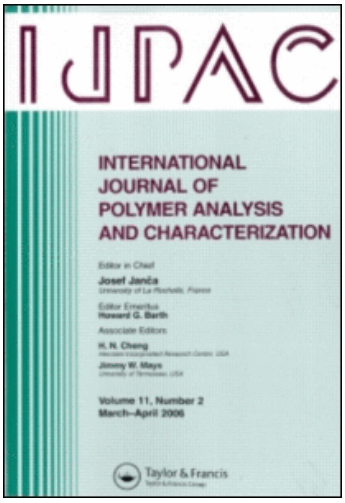

International Journal of Polymer Analysis and Characterization
Publication details, including instructions for authors and subscription information:
http://www.informaworld.com/smpp/title~content=t713646643

Polysaccharide Characterization by Flow Field-Flow Fractionation-Multiangle Light Scattering: Initial Studies of Modified Starches

Bengt Wittgren[a]; Karl-Gustav Wahlund[a]; Mats Andersson[a]; Cecilia Arfvidsson[a]
[a] Division of Technical Analytical Chemistry, Centre for Chemistry and Chemical Engineering, Lund University, Lund, Sweden

Online publication date: 27 October 2010

To cite this Article Wittgren, Bengt , Wahlund, Karl-Gustav , Andersson, Mats and Arfvidsson, Cecilia(2002) 'Polysaccharide Characterization by Flow Field-Flow Fractionation-Multiangle Light Scattering: Initial Studies of Modified Starches', International Journal of Polymer Analysis and Characterization, 7: 1, 19 — 40
To link to this Article: DOI: 10.1080/10236660214599
URL: http://dx.doi.org/10.1080/10236660214599

International Journal of Polymer Anal. Charact., 7: 19–40, 2002

1023-666X/02 $12.00+.00

Polysaccharide Characterization by Flow Field-Flow Fractionation-Multiangle Light Scattering: Initial Studies of Modified Starches

Bengt Wittgren, Karl-Gustav Wahlund, Mats Andersson, and Cecilia Arfvidsson
Division of Technical Analytical Chemistry, Centre for Chemistry and Chemical Engineering, Lund University, Lund, Sweden

Chemically modified starches are commonly used for various purposes. Depending on the type of derivatization, a chemical degradation of the original polymeric structure may occur, resulting in a change of molar mass. It is therefore always of interest to know the molar mass and possibly the conformation of the derivative. Four commercially available hydroxypropyl and hydroxyethyl modified starches were examined by asymmetrical flow field-flow fractionation combined with multiangle laser light scattering. The weight-average molar mass and the molar mass distribution were determined, with emphasis put on the rapid analysis and studies of the suitable experimental conditions regarding flow rates so that accurate data were obtained. The molar mass distribution determinations showed good reproducibility and repeatability and were fast. Efforts to obtain conformational information are described.

Keywords: Field-flow fractionation; Multiangle light scattering; Modified starches; Polysaccharides; Molar mass distribution

Received 3 April 2000; accepted 25 August 2000.

This study was supported by grants from the Swedish Research Council for Engineering Sciences and SCA Research AB. The development of the flow FFF system was made possible by grants from AstraZeneca R&D Mölndal, the Carl Trygger Foundation, and the Crafoord Foundation. Mr. Åke Ståhl is gratefully acknowledged for supplying the samples.

Address correspondence to Bengt Wittgren, AstraZeneca R&D Mölndal, SE-431 83 Mölndal, Sweden.

Chemically modified starches are commonly used for various purposes, often in connection with the food and pharmaceutical industries, but also for technical and biotechnical applications in other areas. Hydroxyalkylation is one example of a very common modification. Depending on the kind of derivatization, a chemical degradation of the original polymeric structure of the starch may occur and is reflected in a large change of the molar mass. Sometimes the molar mass is intentionally reduced by chemical treatment such as hydrolysis followed by suitable derivatization. It is therefore always of interest to determine the molar mass, and possibly the molecular conformation, as a part of the characterization of the final product.

The molar mass and its distribution have often been determined by size exclusion chromatography (SEC) in combination with a refractive index (RI) detector using some calibration procedure where reference compounds of a chemical and physical nature more or less close to the sample compounds are used[1]. The accuracy of these results depends largely on the choice of suitable reference compounds (''molar mass standards'') having well-known molar masses. In the polysaccharide area, dextrans and pullulans are the reference compounds available. Improvements in the molar mass determinations have been obtained by adding an on-line light scattering detector to the SEC-RI system. Low-angle laser light scattering (LALLS) detectors have been available for a long time, while multiangle light scattering (MALS) instruments became available more recently[2]. The advantage of both is that they permit an absolute measurement of the molar mass because reference compounds are not needed. Hence, the accuracy in determination of molar masses is vastly improved.

With the advent of flow field-flow fractionation (flow FFF) a new tool is available for the size fractionation of water-soluble polymers[3–5]. It allows a flexible adjustment of the experiments to adapt the conditions in the separation channel to a wide range of molecular sizes. When flow FFF is coupled on-line with MALS and RI detectors a flexible and rapid system for molar mass determinations is available[6,7]. Its use for size fractionation and molar mass determination of various polysaccharides has already been demonstrated several times both in symmetrical[6,8,9] and asymmetrical[7,10,11] channels. The unique design termed asymmetrical flow FFF has demonstrated unusually fast fractionations, in the order of 5 min total analysis time, irrespective of the polymer size[7,10,11].

In the present study four commercially available hydroxypropyl and hydroxyethyl modified starches were examined by asymmetrical flow field-flow fractionation combined with multiangle laser light scattering. The samples represent rather common types of modified starch. The aim was to study the possibilities for estimating the weight-average molar mass, the molar mass distribution and molecular size (radius of

gyration) using the instrumental combination of asymmetrical flow FFF-RI-MALS. Emphasis was put on rapid analysis and studies of the suitable experimental conditions regarding flow rates so that accurate data were obtained. The advantages and limitations are discussed.

THEORY

Flow FFF is a size separation method applicable to macromolecular and colloidal material in a wide size range of 1 nm to 50 μm[4]. The separation takes part in thin, flat channels along which a carrier liquid is continuously pumped. The injected sample is transported axially along the channel by this flow. A force acting perpendicular to the channel flow initiates the size fractionation. This force consists of a secondary flow, the so-called crossflow, which compels the sample components to move towards one of the channel walls, the accumulation wall, usually consisting of an ultrafiltration membrane permeable to the flow. This movement, in turn, is counteracted by diffusion, which results in those differently sized sample components differing in their position above the accumulation wall. Due to the parabolic velocity profile of the channel flow, differently positioned components are transported at differing speed. Consequently, there is a separation in time due to differences in diffusion coefficients, i.e., to differences in size and shape.

The basic principles of asymmetrical flow FFF are shown in Figure 1[12]. In this version of flow FFF one wall is permeable to the liquid, whereas the other wall is solid, consisting of a glass plate. Accordingly, the crossflow, which in symmetrical flow FFF is pumped independently through the entire cross-section of the channel, is generated from the part of the channel flow that exits through the membrane. Hence, the inlet flow rate V_{in} is divided into the outlet flow rate V_{out} and the crossflow rate V_c

$$V_{\text{in}} = V_c + V_{\text{out}} \tag{1}$$

The level of retention of a component, defined as the ratio of the retention time t_r to the void time t^0, depends directly on V_c so that a higher level of retention, and thus increased resolution, is achieved by an increase in V_c[12,13].

The determination of molar mass and size using the multiangle light scattering detector is based on the Rayleigh-Gans-Debye approximation of static light scattering[2]. By measurements of the scattering intensity (i.e., the Rayleigh ratio R_θ) in each small slice i of the fractionated sample the molar mass M_i can be derived from

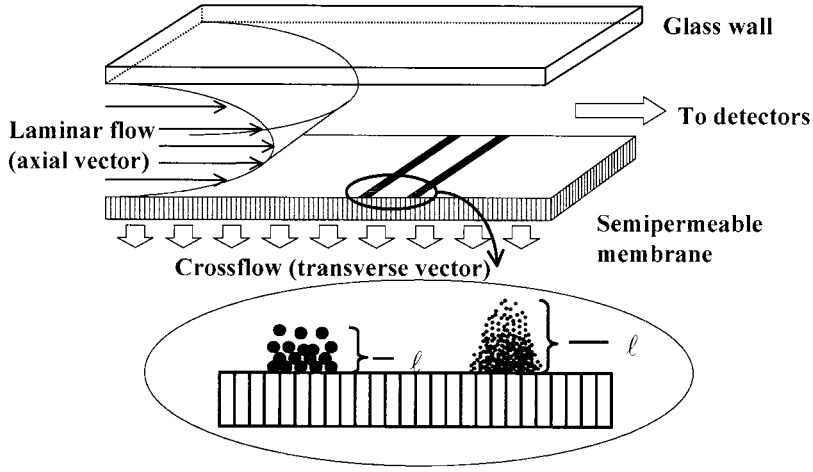

FIGURE 1 The principle of asymmetrical flow FFF. The carrier flow with a parabolic velocity profile is pumped along the channel. The sample components are influenced both by the channel flow (the axial vector), which transports them in the axial direction to the detector, and the cross flow (the transverse vector), which presses them towards the membrane. The separation in time is dependent on position of the center of mass *l*, which in turn is determined by the diffusion coefficient of each component.

$$\frac{Kc_i}{R_{\theta_i}} = \left[\frac{1}{P(\theta)_i}\right]\left[\frac{1}{M_i} + 2A_2c\right] \tag{2}$$

where c is the sample concentration, A_2 is the second virial coefficient, M is the molar mass, θ is the scattering angle and K an instrumental constant. The form factor $P(\theta)$, which is connected to the root-mean-square radius (or more commonly the radius of gyration) r_G, is usually given in its reciprocal form

$$P(\theta)_i^{-1} = 1 + \frac{16\pi^2\langle {r_G}^2\rangle_{z_i}}{3{\lambda_0}^2}\sin^2\left(\frac{\theta}{2}\right) \tag{3}$$

where λ_0 is the wavelength of the light. For small macromolecules having an r_G typically below 10 nm, the angular dependence of the scattering of light will be very weak. Thus, $P(\theta)$ will approach unity and information regarding r_G, according to equation (3), will not be accessible.

The concentration of the polymer in each slice is determined simultaneously by an inline concentration detector, e.g., a refractive index

detector. This allows both distributions and averages to be obtained for both the molar mass and the radius of gyration[2,7]. Consequently, the polydispersity index, M_w/M_n, an important parameter in polymer characterization, can also be obtained from the flow FFF-MALS measurements. One should note that the accuracy in the obtained distribution of molar mass and size depends strictly on the quality of the separation. MALS determines the average molar mass and size for every separated slice of the peak, and these averages could represent a broad distribution of sizes when the separation is poor. Thus, care should be taken to optimize separation conditions to ensure reliable information concerning distributions and averages.

EXPERIMENTAL

Materials

Four starch samples were examined. They were hydroxyethyl starch (HES), Aquaphase PPT, REPPAL PES 100 and REPPAL PES 200, all kindly supplied by Mr. Å. Ståhl at Carbamyl AB (Karlshamn, Sweden). HES (McGaw, Inc., Irvine, California) was obtained from "waxy" starch almost entirely composed of amylopectin. After the hydroxyethyl ether groups have been substituted into the starch the resulting material has been hydrolyzed to yield a suitable molar mass. The weight-average molar mass was reported by the manufacturer to be 458,012, with 80% of the polymers falling in the range of 48,456, to 1,195,363, as determined by high performance size exclusion chromatography combined with low-angle or multiangle light scattering. Aquaphase PPT (Reppe Glykos AB, Växjö, Sweden) is a hydroxypropyl starch (degree of substitution, DS = 0.12) that has been enzymatically converted. The weight-average molar mass was expected to be about 100,000. REPPAL PES 100 (Carbamyl AB, Karlshamn, Sweden) is a hydroxypropyl starch (DS = 0.15) converted by acid hydrolysis to reduce the molar mass. The manufacturer reported a weight-average molar mass of 126,000 determined by gel filtration with RI detection and calibration versus dextran standards. REPPAL PES 200 is also an acid-converted hydroxypropyl starch (DS = 0.15) but with a higher reported weight-average molar mass of 196,000. All samples were spray-dried and therefore soluble in cold water. The water content in the samples was 4–6%.

An in-house-constructed asymmetrical flow FFF instrumental setup was used. It has been described in detail previously[10,11]. To this instrument, a Dawn DSP multiangle laser light scattering instrument (Wyatt Technology Corp., Santa Barbara, California) was coupled on-

line followed by an Optilab DSP refractive index detector (Wyatt Technology Corp., Santa Barbara, California) (Figure 2).

The accumulation wall was a regenerated cellulose ultrafiltration membrane (UF-C10, Hoechst) with a molar mass cutoff of 10,000 as defined by the manufacturer from experiments with globular proteins. The spacer was 130 μm thick and cut out from a poly(methylmetacrylate) film. The sample injection volume was 20 μL. The dimension of the channel was 28.5 cm in length and with a width decreasing from 2.0 to 0.5 cm[13].

The carrier solvent was filtered through a 0.2 μm filter and then degassed by ultrasonication. All water used was purified in a MilliQ water purification system and all chemicals were of analytical grade or better.

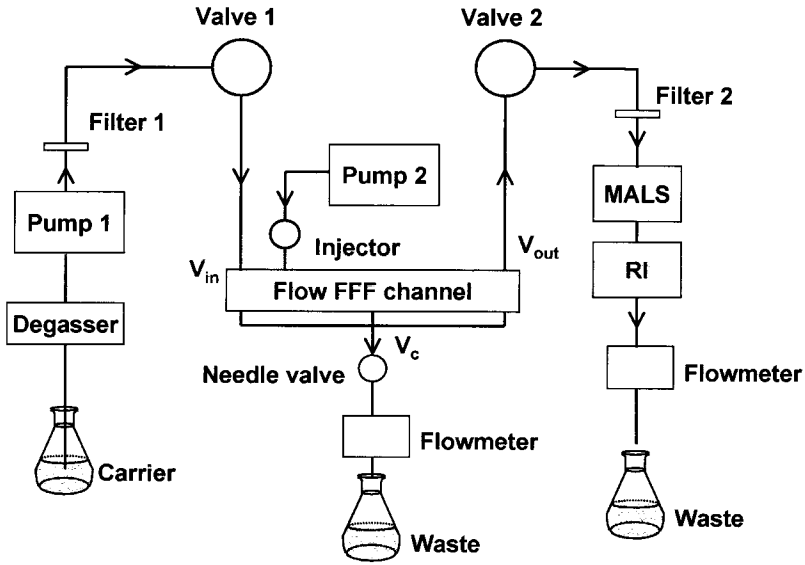

FIGURE 2 A schematic drawing of the asymmetrical flow FFF-MALS system. The arrows indicate the flow directions during the elution phase. The two detectors, MALS and RI, are connected to the channel outlet via the inline filter 2 (pore size 0.45 μm). The carrier flow from pump 1 is purified by the inline filter 1 (pore size 0.02 μm). Pump 2 is used only for injecting the sample into the separation channel. The crossflow rate (V_c) versus the outlet flow rate (V_{out}) is adjusted by a needle valve and both V_c and V_{out} are continuously measured by a flow meter.

Methods

The experimental setup and procedures for asymmetrical flow FFF-MALS-RI were identical to a previous study and will not be further described here except where deviations exist.

Refractive index increments, dn/dc, were determined by the DNDC5 software (Wyatt Technology Corp., Santa Barbara, California). The samples were dissolved in 0.1 M NaCl at room temperature and then kept in a refrigerator overnight. The measurements were performed the day after at room temperature using a flow rate of 0.5 mL/min. The injected sample volume was 1 mL and seven different sample concentrations in the range 4×10^{-5}–30×10^{-5} g/mL were used. The following dn/dc data were obtained: 0.153 for HES, 0.144 for Aquaphase PPT, 0.155 for REPPAL PES 100 and 0.156 for REPPAL PES 200. The concentration values were uncorrected for the water content in the starch samples.

For asymmetrical flow FFF-MALS-RI experiments, the modified starch samples were dissolved directly in the FFF carrier solvent, 0.1 M NaCl containing 0.02% sodium azide, at three different concentration levels: 2, 5 and 10 mg/mL. The freshly made sample was kept overnight in a refrigerator and then analyzed within two days.

The sample injection time in the flow FFF channel was 25 s and the following relaxation/focusing time was 35 s. During the sample injection/relaxation/focusing a valve on the crossflow outlet tubing exiting from the channel was opened to the atmosphere so as to bypass the needle valve, hereby reducing the pressure in the channel. Before the start of the elution phase this valve was closed again. The channel inlet flow rate, V_{in}, was either 2.0 or 3.0 mL/min. The channel outlet flow rate was kept constant at 1.0 ± 0.04 mL/min, which means that the crossflow rate was either 1.0 or 2.0 mL/min, respectively.

The recovery was determined from the integrated RI-signal in relation to the known mass of sample injected to the flow FFF-MALS-RI.

RESULTS AND DISCUSSION

The combination of asymmetrical flow FFF and MALS provides an efficient method of determining molar mass and its distribution for water-soluble polymers. Asymmetrical flow FFF separates components based on their differences in diffusion coefficients, and thereby the hydrodynamic radius. It allows rapid size fractionation using aqueous carrier media with a rather free choice of the carrier composition (salts, buffers, etc.). The MALS in combination with the RI gives the possibility to measure the molar mass and the radius of gyration (root-mean-square radius) across the size spectrum in the separated fractions. Thus various

averages of molar mass, the molar mass distribution and conformational information can be gathered. However, the successful application of the methodology depends on the performance and limitations of the experiments and the instrumentation. For example, to determine the molar mass distribution of a polymer, its components have to be well separated with respect to their molar masses. This puts demands on the resolution in the fractionation procedure. It also requires that the fractionation is effective in the molar mass range covered by the sample. While there is essentially no, or at least a very high, upper size limit in flow FFF, the presence of the ultrafiltration membrane used as the accumulation wall sets a lower size limit because the flow FFF channel can retain only those polymeric components that are larger than the cutoff of the membrane. In this study we have used a cellulosic membrane with a cutoff of 10,000 g/mol.

Further, when it comes to the MALS measurements, a value for the refractive index increment of the polymer studied is required and the possibilities for evaluating molar masses depend on the available concentration of the polymer as well as the breadth of the molar mass range. The light scattering signal eventually becomes too weak as the molar mass decreases. For extremely high molar masses, an accurate evaluation may become difficult if a nonlinear relationship is obtained in the Debye plots. Since the molar mass measurements require good signal-to-noise ratio both for the MALS and the RI, one can expect limitations at the low molar mass end by the MALS since small molecules give low light scattering intensities. At the high molar mass end, a limitation is the weak RI response caused by the low concentrations while the high molar masses still give strong light scattering signals.

In a flow FFF-MALS-RI experiment important variables will be the flow rates and the sample concentration[10]. The flow rates can be used to adjust the magnitude of the crossflow field and thereby the degree of retention as well as the resolution. A basic requirement will always be that even the smallest polymer chains are well retained so that good resolution is also obtained in the low molar mass end of the size distribution. Flow rates naturally also effect the elution time and therefore the total analysis time. While high sample concentrations are beneficial in detecting the low and high molar mass ends of a size distribution, they may lead to overloading phenomena in the flow FFF channel. These can be manifested in shifts in the elution time and peak shape and, more seriously, a decrease in the resolution. From a flow FFF perspective the sample concentration would therefore always have to be minimized. This situation calls for careful optimization of sample concentrations, and it is advisable to always test a range of sample concentrations before deciding how the analysis should be performed.

In this study, four samples of two commonly occurring types of chemically modified starches were subjected to analysis by asymmetrical

flow FFF-MALS-RI and the molar mass distribution and radius of gyration evaluated. Three of the samples have, according to the manufacturers, weight-average molar masses in the range 100,000–200,000 while the fourth sample was of much higher molar mass, almost 500,000. Because the distributions are expected to be broad, the samples all together should be expected to contain significant amounts of polymer from molar masses of a few thousands up to around a million. This broad range may require different flow rate regimes for each sample in the asymmetrical flow FFF experiments.

Molar mass and size as described above are extracted from the Debye plot, i.e., equation (2) applied on very dilute solutions. This is illustrated for one volume fraction of the high molar mass starch derivative HES in Figure 3. The points in the plot correspond to the scattering intensity (i.e., to the ratio Kc/R_θ) obtained at each scattering angle θ. The molar mass is determined from the intercept of the fitted line whereas the radius of gyration is derived from the slope. The precision and accuracy of these determinations are improved by an increase of the signal-to-noise ratio for the MALS and the RI detectors by using well-filtered solvents and clean detector flow cells. Increase of sample concentration is another way to create high signals but for polymers may easily result in overloading effects such as chain entanglements, which in turn would lead to erroneous size fractionation and results. For HES, as illustrated in Figure 3, the quality of the MALS signals allows all accessible angles except angle 3 to be used in the Debye plot, which increases the precision in the extrapolation to zero angle and thus in the molar mass and in the radius of gyration.

The molar masses obtained for the fractionated HES sample are depicted in Figure 4. Note the very short fractionation time of 5 min. The superimposed RI and MALS responses differ in a characteristic way for broadly distributed polymers. The RI curve typically has its maximum early in the fractogram, at 1 min, whereas the MALS signal peaks at 2 min due to its high sensitivity for large molecules. There is a continuous increase of the molar mass with elution time, which is reasonable regarding the separation order of flow FFF. The opposite order is observed for very short retention times, $t_r < t^0$, which does not correspond to properly fractionated sample components. This is likely an artefact caused partly by a disturbed MALS/RI signal in the very early part of the fractogram directly after the elution starts and should not be included in the calculated molar mass distribution[10]. Likewise, the irregular and noisy molar mass data obtained at the end of the peak should also be excluded since it most probably does not reflect realistic values but is instead an artefact caused by the rather weak RI signal[10]. Thus, there is a range between 40,000 and 3,000,000 g/mol in molar mass that appears to be properly fractionated and analyzed for this sample. A similar approach should be

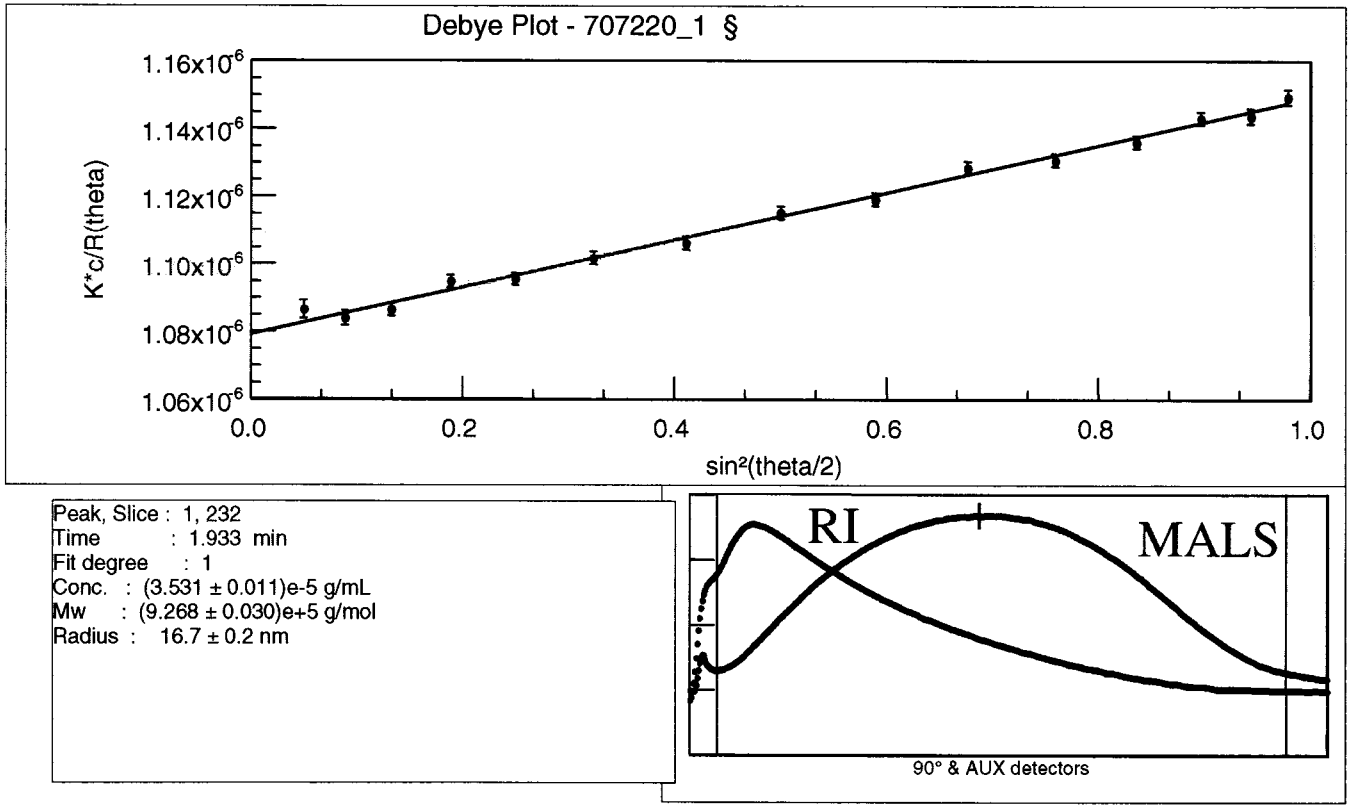

FIGURE 3 The Debye plot obtained for a volume fraction of the HES sample. Angles 4 (26°) to 18 (163°) are used for extraction of the molar mass (from the intercept of the fitted line) and of the radius of gyration (from the slope of the line) according to the Zimm method[2].

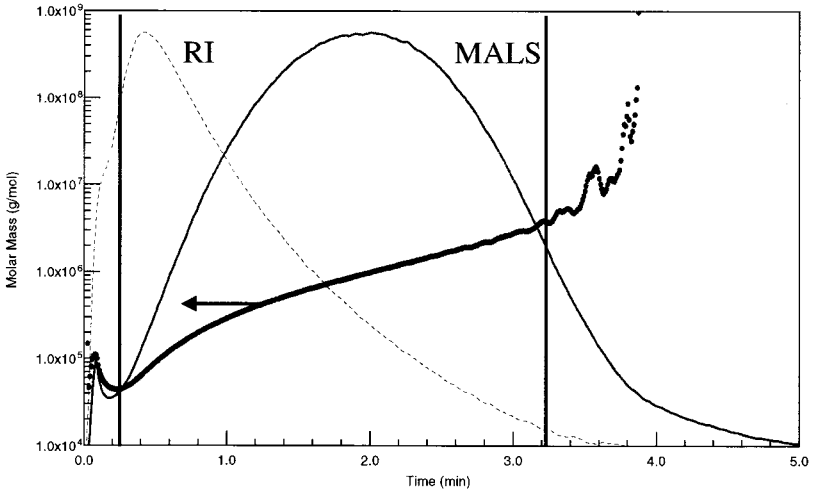

FIGURE 4 RI fractogram (dotted line) and MALS 90° fractogram (solid line) of HES, 10 mg/mL. The calculated molar masses for each slice in the fractionated peak are superimposed. The vertical lines illustrate the part of the peak having reasonable molar mass values and can be used for the molar mass distribution. The crossflow rate $V_c = 2\,\text{mL/min}$ and the outlet flow rate $V_{\text{out}} = 1.0\,\text{mL/min}$.

applied for obtaining a realistic distribution of the radius. The general aim when flow FFF-MALS is employed for determination of molar mass and size is to maximize this range by using proper flow rates and sample concentrations. Such experiments have been performed for the starch derivatives and are discussed below.

Effects of Flow Rates and Sample Concentration

The plot of the molar mass against the retention time for the low molar mass sample Aquaphase obtained at different flow rates and sample concentrations is seen in Figure 5. The lowest sample concentration (Figure 5A), 2 mg/mL, results in a rather narrow range of obtained molar masses, 40,000 to 250,000 g/mol. An increase to 10 mg/mL (Figure 5B) extended the range to 500,000 g/mol, but an increase also in V_c from 1.0 to 2.0 mL/min (Figure 5C) gave a much broader range, from 30,000 to 1,000,000 g/mol. The cumulative molar mass distributions for these analyses are depicted in Figure 6. The experimental conditions used in Figure 6C provided the broadest

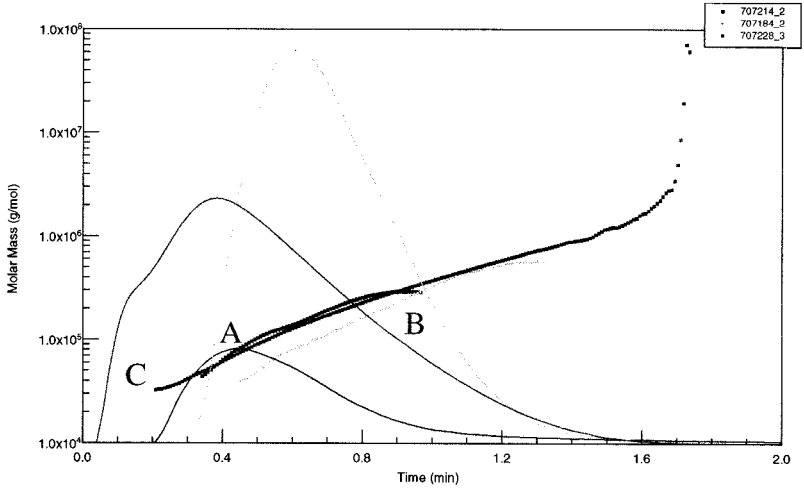

FIGURE 5 The molar mass against the retention time for Aquaphase obtained at three different experimental conditions: A. sample concentration 2 mg/mL, $V_c = 1.0$ mL/min, V_{out} 1.0 mL/min, $t^0 = 0.26$ min; B. sample concentration 10 mg/mL, V_c 1.0 mL/min, V_{out} 1.0 mL/min, $t^0 = 0.26$ min and C. sample concentration 10 mg/mL, V_c 2.0 mL/min, V_{out} 1.0 mL/min, $t^0 = 0.21$ min.

distribution and thus the highest polydispersity index, M_w/M_n, 1.6 (Table I). The M_w increased to be about 180,000 g/mol for the high crossflow rate and the recovery fell from 77 to 60%. Consequently, parts of the sample do not reach the detector, and the distributions seen in Figure 6 therefore do not correspond to the complete sample. In particular, information regarding the low molar mass part of the distribution is lacking due to the interruption at about 30,000–40,000 g/mol. It is not likely that these values represent the lowest molar mass components present in the sample. Smaller material may be lost through the ultrafilter or is too little retained to be properly separated from the void peak. A higher retention level for the low molar mass part of the sample is therefore required but such an increase may, on the other hand, disturb the high molar mass components[10]. The radius of gyration is even more dependent on optimized conditions than is the molar mass due to the lower radius limit of 10 nm for the radius determination measurement. This is crucial for a low molar mass sample like Aquaphase where the angular dependence is rather weak because a major fraction of this sample appear to be of small size (<10 nm), as clearly illustrated in Figure 7. Reasonable results are obtained only in Figure 7C and then solely for the high

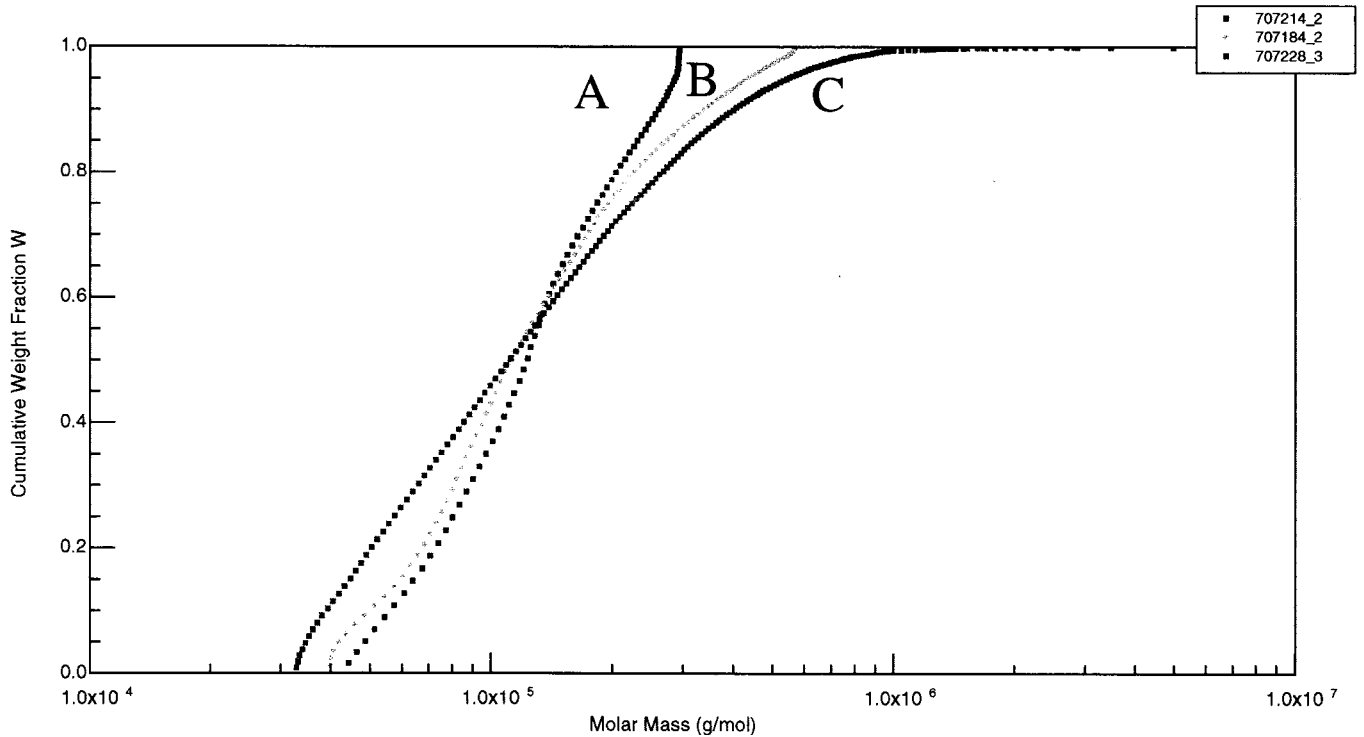

FIGURE 6 The cumulative molar mass distribution for Aquaphase obtained at three different experimental conditions: A. sample concentration 2 mg/mL, $V_c = 1.0$ mL/min, V_{out} 1.0 mL/min, $t^0 = 0.26$ min; B. sample concentration 10 mg/mL, V_c 1.0 mL/min, V_{out} 1.0 mL/min, $t^0 = 0.26$ min and C. sample concentration 10 mg/mL, V_c 2.0 mL/min, V_{out} 1.0 mL/min, $t^0 = 0.21$ min.

TABLE I Concentration and flow-rate effects on molar mass and radii data for the four modified starches.

Sample	Sample concentration (mg/mL)	Crossflow rate (V_c)	M_w	M_w/M_n	r_{Gz} (nm)	Recovery (%)
REPPAL PES 100	2	1.0	158,000	1.9	21	79
	10	1.0	215,000	2.6	14	65
	10	2.0	212,000	2.6	13	66
REPPAL PES 200	2	1.0	n.d.	n.d.	n.d.	n.d.
	10	1.0	275,000	2.1	16	76
	10	2.0	289,000	2.2	14	73
Aquaphase PPT	2	1.0	159,000	1.2	17	81
	10	1.0	166,000	1.6	11	77
	10	2.0	187,000	2.0	8	60
HES	2	1.0	534,000	1.6	15	84
	10	1.0	547,000	2.8	20	89
	10	2.0	564,000	3.3	20	84

molar mass part of the distribution. The conclusion is that meaningful radii distributions for this low molar mass sample are not available. Similar results were obtained also with the other two low molar mass samples, PES 100 and PES 200.

The data for the high molar mass sample, HES, are also influenced by the experimental conditions largely in the same way as the Aquaphase sample. Clearly, the high concentration provided a broader, more reliable molar mass distribution (Figures 8B, 8C and Figures 9B, 9C). The polydispersity index (Table I) ranged from 1.6 obtained for condition A in Figure 8 to 2.8 for condition B, which confirms the strong influence of the sample concentrations. The usual drawbacks connected to high sample concentrations such as possible chain entanglement leading to low recovery[10] and skew peaks[14] are not observed here. The difference between the high and low crossflow rates is much less pronounced than for the Aquaphase sample. This is likely explained by the presence of larger components in HES being better resolved also at the low crossflow rate (1.0 mL/min). Another effect of having larger components is the precision in the radii-of-gyration data being much improved over a broader range of the molar mass distribution, at least at high sample concentrations (Figure 10B and C). The analysis performed at high concentration and high crossflow rate (Figure 10C) provided a radii range of between 8 and 30 nm. Radii below 8 nm most probably also exist in the distribution but are difficult to extract from the very weak angular dependence at this level.

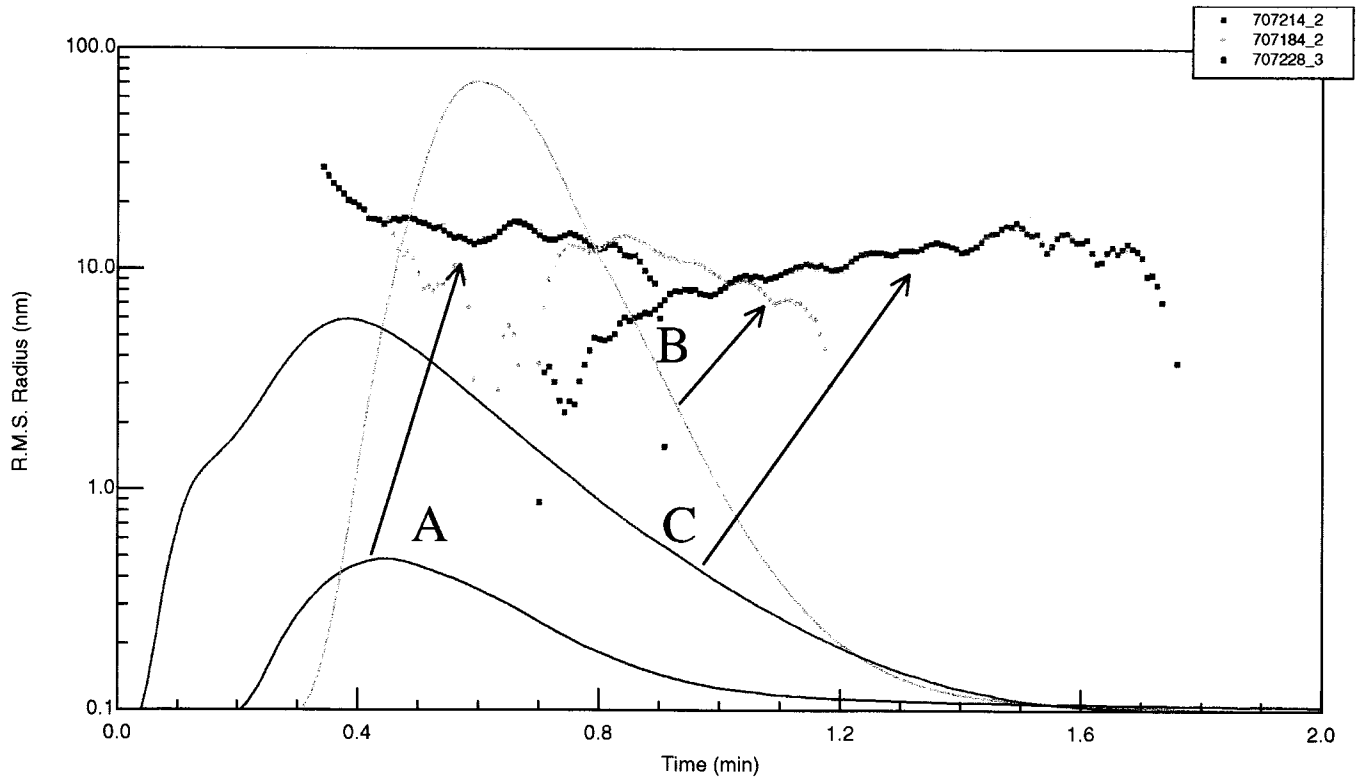

FIGURE 7 The radius of gyration against the retention time for Aquaphase obtained at three different experimental conditions: A. sample concentration 2 mg/mL, $V_c = 1.0$ mL/min, V_{out} 1.0 mL/min, $t^0 = 0.26$ min; B. sample concentration 10 mg/mL, V_c 1.0 mL/min, V_{out} 1.0 mL/min, $t^0 = 0.26$ min and C. sample concentration 10 mg/mL, V_c 2.0 mL/min, V_{out} 1.0 mL/min, $t^0 = 0.21$ min.

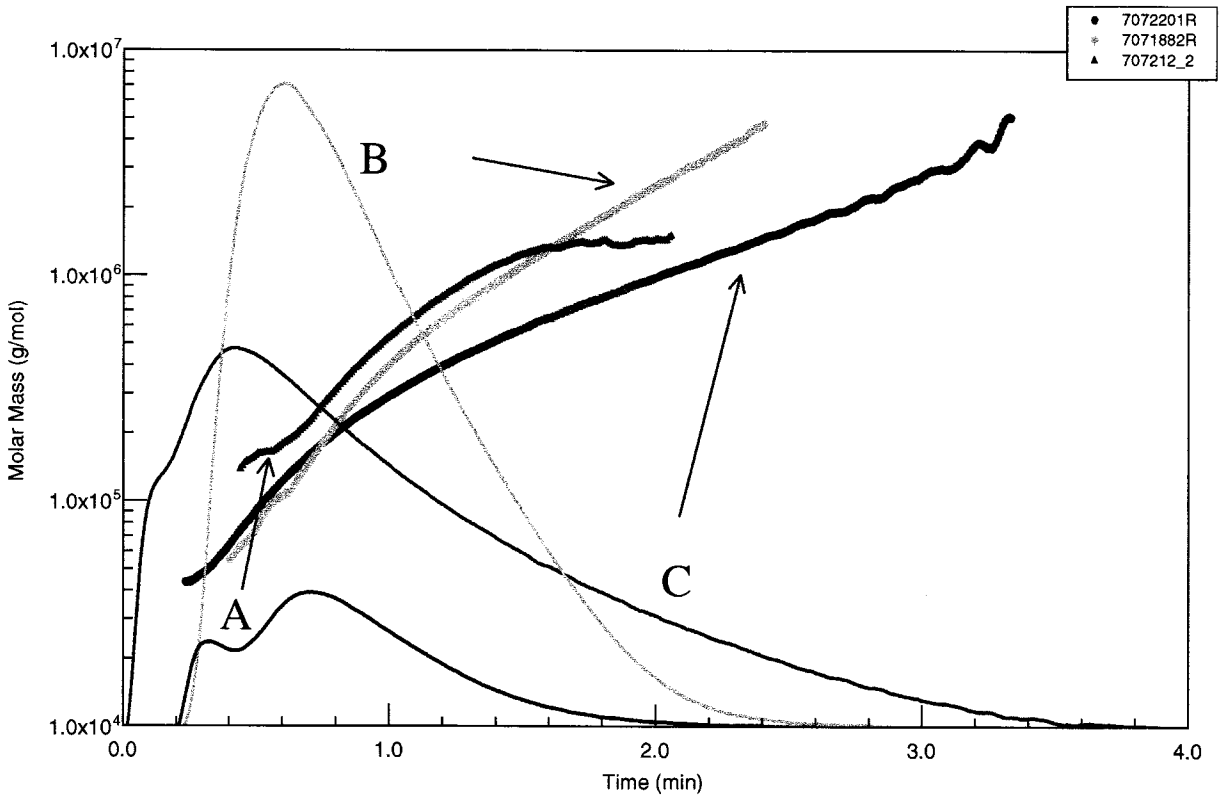

FIGURE 8 The molar mass against the retention time for HES obtained at three different experimental conditions: A. sample concentration 2 mg/mL, $V_c = 1.0$ mL/min, V_{out} 1.0 mL/min, $t^0 = 0.26$ min; B. sample concentration 10 mg/mL, V_c 1.0 mL/min, V_{out} 1.0 mL/min, $t^0 = 0.26$ min and C. sample concentration 10 mg/mL, V_c 2.0 mL/min, V_{out} 1.0 mL/min, $t^0 = 0.21$ min.

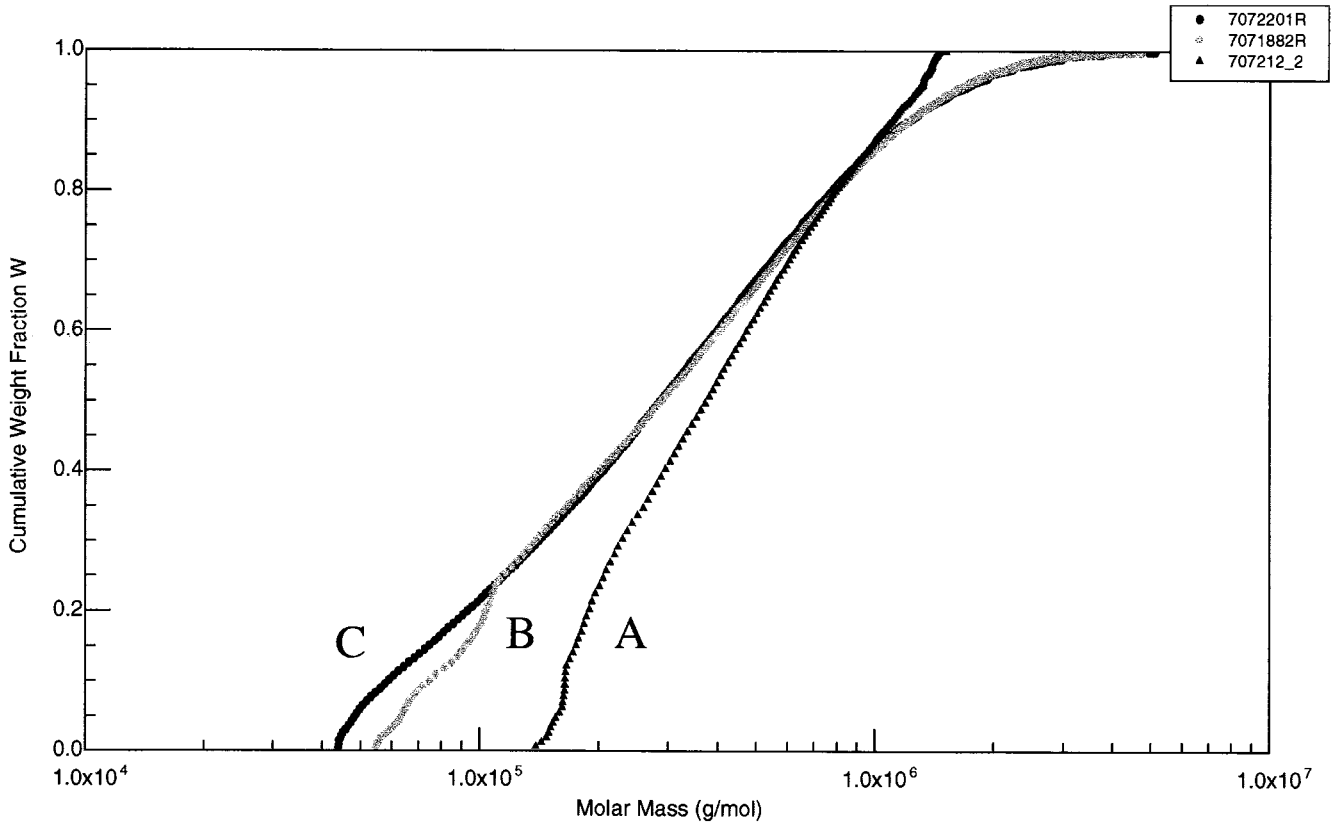

FIGURE 9 The cumulative molar mass distribution of HES obtained at three different experimental conditions: A. sample concentration 2 mg/mL, $V_c = 1.0$ mL/min, V_{out} 1.0 mL/min, $t^0 = 0.26$ min; B. sample concentration 10 mg/mL, V_c 1.0 mL/min, V_{out} 1.0 mL/min, $t^0 = 0.26$ min and C. sample concentration 10 mg/mL, V_c 2.0 mL/min, V_{out} 1.0 mL/min, $t^0 = 0.21$ min.

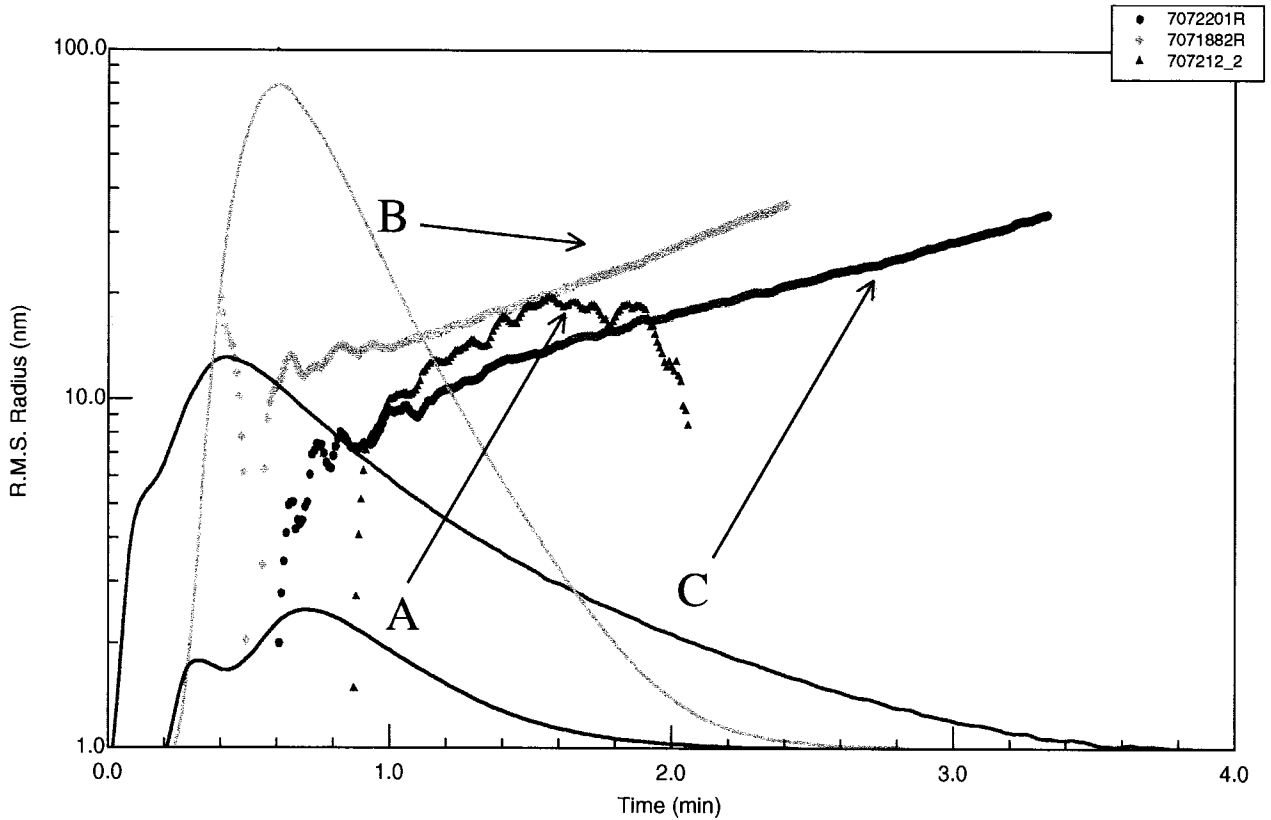

FIGURE 10 The radius of gyration against the retention time for HES obtained at three different experimental conditions: A. sample concentration 2 mg/mL, $V_c = 1.0$ mL/min, V_{out} 1.0 mL/min, $t^0 = 0.26$ min; B. sample concentration 10 mg/mL, V_c 1.0 mL/min, V_{out} 1.0 mL/min, $t^0 = 0.26$ min and C. sample concentration 10 mg/mL, V_c 2.0 mL/min, V_{out} 1.0 mL/min, $t^0 = 0.21$ min.

Molar Mass, Size and Conformation

The experiments performed at different flow rates and sample concentrations belong to compulsory procedures in polymer characterization using flow FFF-MALS. Preferred conditions appear to be the high sample concentration (10 mg/mL) and the high crossflow rate (2 mL/min) for all four starch derivatives. Results obtained under these conditions are gathered in Table II. The molar mass distributions for the four samples are displayed in Figure 11. The high molar mass HES sample reaches a weight-average molar mass of 564,000 compared to 187,000 for the Aquaphase sample. All four samples have quite broad molar mass distributions with polydispersity indices between 2.0 and 3.4. However, the M_w values provided by flow FFF-MALS are significantly higher for all four samples in comparison to the manufacturers' data. It seems likely that this is an effect of low-molar-mass components either disappearing through the ultrafilter or not being retained enough to be included in the calculated distribution. It would further explain the low recovery observed—especially for the low molar mass samples. Due to the limitations of MALS itself the radii data presented in Table II correspond only to those polymers in the distribution having radii larger than approximately 8 nm. Thus, the reported data do not reflect the complete sample. Further studies using ultrafilters having lower cutoffs, higher crossflows and more sensitive MALS instruments may provide a more complete picture of these very broad distributions.

Since information on both molar mass and size distributions are simultaneously provided by flow FFF-MALS, it is possible to construct double logarithm plots of molar mass versus radius of gyration[2]. The slope from such a plot depends on the actual conformation where 0.33 relates to a spherical shape and 0.5 to a random coil in theta solvent. Due

TABLE II Molar mass averages, polydispersity and root-mean-square radius (radius of gyration) for modified starches obtained under best possible conditions.

Sample	M_w (manufacturer's data)	M_w	M_w/M_n	r_{Gz} (nm)	Conformational parameter	Recovery (%)
HES	458,000	564,000	3.3	20	0.44	84
Aquaphase PPT	107,000	187,000	2.0	8	n.d.[a]	60
REPPAL PES 100	129,000	212,000	2.6	13	n.d.	66
REPPAL PES 200	196,000	289,000	2.2	12	n.d.	69

[a] Not determined

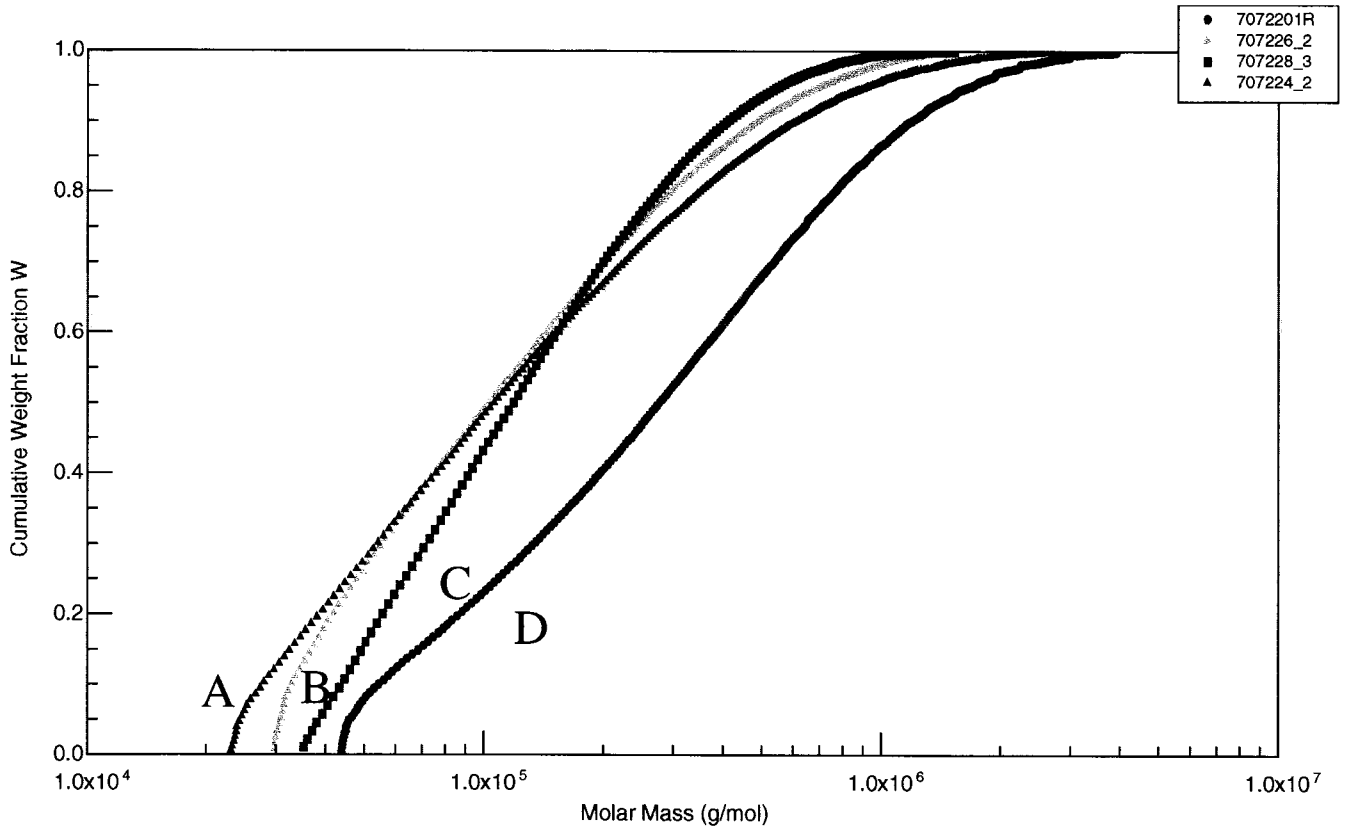

FIGURE 11 The cumulative molar mass distribution obtained for A. PES 200, B. PES 100, C. Aquaphase and D. HES.

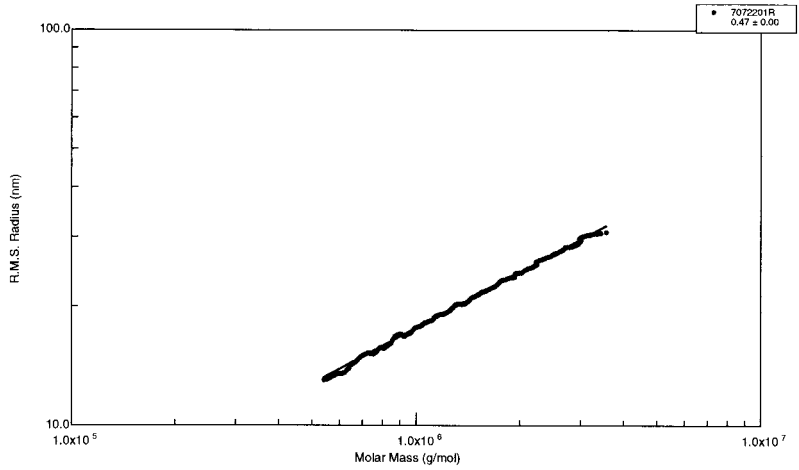

FIGURE 12 Plot of the radius of gyration versus the molar mass (conformation plot) for the HES sample in the molar mass interval of 500,000 to 3,000,000 g/mol. The slope was 0.47.

to the relatively small sizes of the starch derivatives studied, it was difficult to get information about the conformation for all of them. For HES, having the broadest range of reliable molar mass and radii, information regarding the conformation is at hand (Figure 12). A consistent slope of 0.47 is obtained in the molar mass range of 400,000 to 3,000,000. However, since the available molar mass range corresponds to only 30% of the HES, the obtained conformation is not representative for the whole sample. Thus, further experiments emphasizing the increased information of low molar mass material are needed.

CONCLUSION

This study has demonstrated that flow FFF in combination with MALS has the capability of performing a rapid size characterization of modified starches. A careful examination of various sample concentrations and flow rates is clearly shown to be a necessary step towards reliable results. Nevertheless, flow FFF-MALS overestimates the weight-average molar mass especially of the three low-molar-mass starches. Most probably, this reflects the difficulties of properly characterizing the low-molar-mass components present in the wide molar mass distributions of these samples. Even a loss of smaller macromolecules through the ultrafiltration membrane is probable, considering the low recovery

observed. The use of ultrafilters with lower cutoffs may thus be one way to improve the recovery and thereby obtain results for the complete molar mass distribution. For the high molar mass sample, HES, the recovery is acceptable, 84%. The *z*-average radius of gyration of this sample, 20 nm, is low in comparison with the weight-average molar mass 564,000 g/mol, suggesting a rather compact conformation. The same conclusion can be drawn from the conformation plot, which seems reasonable considering the branched structure of amylopectin.

REFERENCES

[1] Harding, S. E., Varum, K. M., Stokke, B. T. and Smidsrod, O. (1991). *Adv. Carbohydr. Anal.*, **1**, 63.
[2] Wyatt, P. J. (1993). *Anal. Chim. Acta.*, **272**, 1.
[3] Giddings, J. C. and Benincasa, M. A. (1992). *Anal. Chem.*, **64**, 790.
[4] Giddings, J. C. (1993). *Science*, **260**, 1456.
[5] Wittgren, B., Wahlund, K.-G., Derand, H. and Wesslén, B. (1996). *Macromolecules*, **29**, 268.
[6] Roessner, D. and Kulicke, W.-M. (1994). *J Chromatogr. A*, **687**, 249.
[7] Wittgren, B. and Wahlund, K.-G. (1997). *J Chromatogr. A*, **760**, 205.
[8] Thielking, H. and Kulicke, W.-M. (1996). *Anal. Chem.*, **68**, 1169.
[9] Adolphi, U. and Kulicke, W. M. (1997). *Polymer*, **38**, 1513.
[10] Wittgren, B. and Wahlund, K.-G. (1997). *J. Chromatogr. A*, **791**, 135.
[11] Wittgren, B., Borgström J., Wahlund, K.-G. and Piculell, L. (1998). *Biopolymers*, **45**, 85.
[12] Wahlund, K.-G. and Giddings, J. C. (1987). *Anal. Chem.*, **59**, 1332.
[13] Litzén, A. and Wahlund, K.-G. (1991). *Anal. Chem.*, **63**, 1001.
[14] Caldwell, K. D., Brimhall, S. L., Gao, Y. and Giddings, J. C. (1988). *J. Appl. Polym. Sci.*, **36**, 703.